Multi-stability of free spontaneously curved anisotropic strips

L. Giomi and L. Mahadevan

References	**This article cites 16 articles, 5 of which can be accessed free** http://rspa.royalsocietypublishing.org/content/468/2138/511.full.html#ref-list-1
Subject collections	Articles on similar topics can be found in the following collections applied mathematics (252 articles) mechanics (94 articles)
Email alerting service	Receive free email alerts when new articles cite this article - sign up in the box at the top right-hand corner of the article or click **here**

To subscribe to *Proc. R. Soc. A* go to: **http://rspa.royalsocietypublishing.org/subscriptions**

Multi-stability of free spontaneously curved anisotropic strips

BY L. GIOMI* AND L. MAHADEVAN

Department of Physics, School of Engineering and Applied Sciences, Harvard University, Pierce Hall 29 Oxford Street, Cambridge, MA 02138, USA

Multi-stable structures are objects with more than one stable conformation, exemplified by the simple switch. Continuum versions are often elastic composite plates or shells, such as the common measuring tape or the slap bracelet, both of which exhibit two stable configurations: rolled and unrolled. Here, we consider the energy landscape of a general class of multi-stable anisotropic strips with spontaneous Gaussian curvature. We show that while strips with non-zero Gaussian curvature can be bistable, and strips with positive spontaneous curvature are always bistable, independent of the elastic moduli, strips of spontaneous negative curvature are bistable only in the presence of spontaneous twist and when certain conditions on the relative stiffness of the strip in tension and shear are satisfied. Furthermore, anisotropic strips can become tristable when their bending rigidity is small. Our study complements and extends the theory of multi-stability in anisotropic shells and suggests new design criteria for these structures.

Keywords: bistable shells; morphing structures; Gaussian curvature

1. Introduction

The notion of elastic *multi-stability* has drawn considerable attention in the past few years owing to the potential for the design of smart structures. A multi-stable structure is an elastic object (typically a fibre-reinforced composite) that exhibits more than one equilibrium conformation and can thus be arranged in a variety of shapes without inducing permanent deformations and with no need of mechanical hinges. Everyday examples of these include snapping hair-clips, the slap-bracelet and various jumping toys. Unlike more conventional engineering structures, where large deformations must be accompanied by large forces, multi-stable objects can switch between shapes using a small actuation force. This latter feature has made multi-stable structures promising candidates for the realization of a new generation of adaptive devices, in which these 'morphing' capabilities, combined with limited actuation, allow for switchable, controllable conformational changes. Examples of this new generation of devices are shape-changing mirrors for adaptive focusing in optical

*Author for correspondence (lgiomi@seas.harvard.edu).

511

systems or morphing aircraft structures that can continuously readjust their shape to optimize aerodynamic function (Abdulrahim *et al.* 2005; Mattioni *et al.* 2007).

The quest for a theoretical description of elastic multi-stability dates back to the 1920s when deployable devices, such as the measuring tape, first made their appearance. In this context, it is amusing to note that A. E. H. Love, the author of the classical treatise on elasticity (Love 1927), was once challenged to explain why the longitudinal curvature of a spring-steel measuring tape appears to match exactly its transverse curvature (Petroski 2004). He did not; indeed such an explanation was offered only decades later by Rimrott (1965) and reviewed and distilled into an elegant solution by Calladine (1988). Over the last decade, the work of Iqbal *et al.* (2000), Galletly & Guest (2004*a*,*b*) and Guest & Pellegrino (2006) simplified and clarified the elasticity of bistable objects, unravelling the interplay between anisotropy and spontaneous curvature in determining the shape of bistable plates. Guest & Pellegrino (2006) used a beam model of a strip of infinite length and finite width endowed with constant spontaneous curvature along the transverse direction. Assuming inextensibility, these authors showed that orthotropic strips exhibit a secondary equilibrium conformation in addition to the base configuration. The stability of such a secondary minimum of the elastic energy depends on the relative magnitude of the bending stiffness in the longitudinal and transverse directions as well as the twisting stiffness of the strip. Later, Seffen (2007) considered an extensible elliptical plate with free boundaries and non-zero, constant spontaneous principal curvatures and showed that even isotropic shells might be bistable. More recently, Vidoli & Maurini (2009) extended Seffen's uniform curvature model and showed that two-dimensional orthotropic plates with initial shallow double curvature are in fact *tristable* in some range of elastic moduli and spontaneous curvatures, while a one-parameter family of continuously variable neutrally stable shapes was reported by Seffen & Guest (2011) in the context of prestressed shells.

In this paper, we complement these different results to understand the phase space for multi-stability in spontaneously curved elastic strips, but lift the assumptions of inextensibility and uniform curvature, with the goal of analysing an entire range of morphing scenarios (including tristability) without compromising the simplicity of the analytical treatment. Our system consists of a free anisotropic elastic strip with spontaneous double curvature and, in general, spontaneous twist. In this setting, we look for a general solution without assuming deformations to be inextensible or the curvature to be constant across the strip. This latter feature, in particular, is what makes tristability possible, even in the reduced dimensionality of strip-like plates and allows us to map a 'phase diagram' for the existence of bi- and tristability. In §2, we present the fundamental equations describing general anisotropic elastic strips following the approach of Mansfield (1973), Reissner (1992) and most recently, Galletly & Guest (2004*b*), who considered the specific case of composite bistable tubes. In §3, we specialize our analysis to the case of orthotropic strips and discuss the associated energy landscape. In §4, we briefly discuss the case of strips with coupling between stretching and bending, highlighting the differences and similarities with orthotropic strips. Section 5 concludes the paper with a focus on open problems and applications.
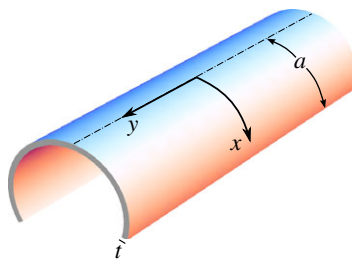
Figure 1. Schematic of a two-dimensional strip of thickness t and width $2a$. The transverse and longitudinal directions are labelled as x and y, respectively. For strips that are six times longer than they are wider, it is sufficient to consider them as effectively infinite along the y direction. (Online version in colour.)

2. Elasticity of anisotropic strips

(a) Formulation

We start by considering a long rectangular plate whose length is much larger than its width $2a$, with x being the coordinate along the direction parallel to the short edge and y the coordinate along the direction parallel to the long edge (figure 1). In practice, we can consider the strip infinite along the y direction to avoid dealing with end conditions. As noted by Mansfield (1973), strips with aspect ratio five or more are already well described by this approximation.

The general constitutive equations for anisotropic plates can be expressed in terms of the **ABD** matrix (Ashton & Whitney 1970; Jones 1999), that relates the in-plane stresses $\mathbf{N} = (N_x, N_y, N_{xy})$ and out-of-plane moments $\mathbf{M} = (M_x, M_y, M_{xy})$ with the strain $\boldsymbol{\epsilon} = (\epsilon_x, \epsilon_y, \epsilon_{xy})$ and the difference $\boldsymbol{\chi} = \boldsymbol{\kappa} - \mathbf{c}$ between the middle-surface curvatures[1] $\boldsymbol{\kappa} = (\kappa_x, \kappa_y, \kappa_{xy})$ and their preferred (spontaneous) values $\mathbf{c} = (c_x, c_y, c_{xy})$, so that

$$\begin{pmatrix} \mathbf{N} \\ \mathbf{M} \end{pmatrix} = \begin{pmatrix} \mathbf{A} & \mathbf{B} \\ \mathbf{B} & \mathbf{D} \end{pmatrix} \begin{pmatrix} \boldsymbol{\epsilon} \\ \boldsymbol{\chi} \end{pmatrix}, \tag{2.1}$$

where $\mathbf{A}$ represents the extensional stiffness matrix, $\mathbf{D}$ is the bending stiffness matrix and $\mathbf{B}$ embodies the possible coupling between stretching and bending owing to material anisotropy.

In terms of the strain, curvature and the material properties of the shell, the elastic energy density of a general anisotropic plate is given by Mansfield (1989),

$$u = \tfrac{1}{2}(A_{ij}\epsilon_i\epsilon_j + 2B_{ij}\chi_i\epsilon_j + D_{ij}\chi_i\chi_j), \tag{2.2}$$

where the Einstein convention on repeated indices has been used, and the first and third terms are the stretching and bending energy densities, while the second term characterizes the energy associated with the coupling between bending and

---

[1]We use Reissner's notation for the twisting curvature, $\kappa_{xy} = -2\partial^2 w/\partial x \partial y$, where w is the height of the middle-surface above the xy plane.

stretching. Because it is often useful to know the constitutive equations (2.1) in their semi-inverted form, we write them as

$$\begin{pmatrix} \boldsymbol{\epsilon} \\ \mathbf{M} \end{pmatrix} = \begin{pmatrix} \boldsymbol{\alpha} & \boldsymbol{\beta} \\ -\boldsymbol{\beta}^{\mathrm{T}} & \boldsymbol{\delta} \end{pmatrix} \begin{pmatrix} \mathbf{N} \\ \boldsymbol{\chi} \end{pmatrix}, \tag{2.3}$$

where

$$\boldsymbol{\alpha} = \mathbf{A}^{-1}, \quad \boldsymbol{\beta} = -\mathbf{A}^{-1}\mathbf{B} \quad \text{and} \quad \boldsymbol{\delta} = \mathbf{D} - \mathbf{B}\mathbf{A}^{-1}\mathbf{B}, \tag{2.4}$$

so the energy density (2.2) can be expressed in terms of $\mathbf{N}$ and $\boldsymbol{\chi}$ as

$$u = \tfrac{1}{2}(\alpha_{ij} N_i N_j + \delta_{ij} \chi_i \chi_j). \tag{2.5}$$

In the absence of body forces or external loads, the conditions for kinematical compatibility and mechanical equilibrium translate, respectively, into the following partial differential equations (Calladine 1993):

$$\frac{\partial^2 \epsilon_x}{\partial y^2} - \frac{\partial^2 \epsilon_{xy}}{\partial x \partial y} + \frac{\partial^2 \epsilon_y}{\partial x^2} = -\delta K \tag{2.6a}$$

and

$$\frac{\partial^2 M_x}{\partial x^2} + 2\frac{\partial^2 M_{xy}}{\partial x \partial y} + \frac{\partial^2 M_y}{\partial y^2} = \kappa_x N_x + \kappa_{xy} N_{xy} + \kappa_y N_y, \tag{2.6b}$$

where $\delta K = K - K_0$ is the difference between the Gaussian curvature of the deformed plate, $K = \kappa_x \kappa_y - \kappa_{xy}^2$, and its spontaneous Gaussian curvature, $K_0 = c_x c_y - c_{xy}^2$. The radius of curvature of the strip is assumed to be much smaller than the typical length scale of the deformations (i.e. shallow shell approximation). This allows us to simplify the differential structure of the theory by transforming covariant derivatives into standard partial derivatives. Equations (2.6) are then the classic Föppl–von Kármán plate equations expressed in terms of stress and curvature. Because the strip is assumed to be infinitely long in the y direction, all physical quantities should be invariant with respect to translations along y. Mechanical equilibrium requires $\boldsymbol{\nabla}\cdot\mathbf{N} = 0$, which, together with the condition of translational invariance along y, yields

$$\frac{\partial N_x}{\partial x} = \frac{\partial N_{xy}}{\partial x} = 0.$$

In the absence of applied forces along the edges, this implies $N_x = N_{xy} = 0$. In addition, the Mainardi–Codazzi compatibility equations $\nabla_i \kappa_{jk} = \nabla_k \kappa_{ij}$ yield

$$\frac{\partial \kappa_x}{\partial y} - \frac{\partial \kappa_{xy}}{\partial x} = 0 \quad \text{and} \quad \frac{\partial \kappa_y}{\partial x} - \frac{\partial \kappa_{xy}}{\partial y} = 0,$$

which, together with the condition of translational invariance along y, imply that both κ_y and κ_{xy} are constants. Thus, equations (2.6) simplify to

$$\frac{\partial^2 \epsilon_y}{\partial x^2} = -\delta K \tag{2.7a}$$

and

$$\frac{\partial^2 M_x}{\partial x^2} = \kappa_y N_y. \tag{2.7b}$$

Using the semi-inverted constitutive equations (2.3), one can easily rewrite (2.7) in the form of a single differential equation for the transverse moment M_x. To do this, we start by writing

$$\epsilon_y = \alpha_{22} N_y + \beta_{21} \chi_x + \beta_{22} \chi_y + \beta_{26} \chi_{xy} \qquad (2.8a)$$

and

$$M_x = -\beta_{21} N_y + \delta_{11} \chi_x + \delta_{12} \chi_y + \delta_{16} \chi_{xy}. \qquad (2.8b)$$

Then, inverting (2.8b) and using (2.7b), we get

$$\kappa_x = c_x + \frac{1}{\delta_{11}} \left(M_x + \frac{\beta_{21}}{\kappa_y} \frac{\partial^2 M_x}{\partial x^2} - \delta_{12} \chi_y - \delta_{16} \chi_{xy} \right) \qquad (2.9a)$$

and

$$\frac{\partial^2 \kappa_x}{\partial x^2} = \frac{1}{\delta_{11}} \left(\frac{\partial^2 M_x}{\partial x^2} + \frac{\beta_{21}}{\kappa_y} \frac{\partial^4 M_x}{\partial x^4} \right). \qquad (2.9b)$$

Combining these two equations with (2.7), we finally obtain

$$(\alpha_{22}\delta_{11} + \beta_{21}^2) \frac{\partial^4 M_x}{\partial x^4} + 2\beta_{21}\kappa_y \frac{\partial^2 M_x}{\partial x^2} + \kappa_y^2 M_x$$
$$= \kappa_y \{ \delta_{11}(c_x c_y - c_{xy}^2 + \kappa_{xy}^2) + \kappa_y [\delta_{12}(\kappa_y - c_y) + \delta_{16}(\kappa_{xy} - c_{xy}) - \delta_{11} c_x] \}. \qquad (2.10)$$

The boundary conditions associated with equations (2.7) for a strip with no applied forces and torques at the lateral edges have been discussed by Reissner (1992) and translate into the requirement

$$M_x = \frac{\partial M_x}{\partial x} = 0, \qquad x = \pm a. \qquad (2.11)$$

Together, (2.10) and (2.11) complete the formulation of the boundary-value problem for the behaviour of a long anisotropic strip with spontaneous curvature and twist.

(b) Anisotropy classes

Before we go further, it is useful to review the different form of elastic anisotropy, following the theory of laminates (Jones 1999). Various forms of matrix coupling the in-plane strain to the out-of-plane curvature **B** can be obtained by controlling the relative orientation of the laminae forming the layers of a composite plate. Thus, in a cross-ply fibre-reinforced composite, in which the fibres in each layer are alternatively oriented at 0° and 90° with respect to the y-axis of the strip, one has

$$\mathbf{B} = \begin{pmatrix} B_{11} & 0 & 0 \\ 0 & -B_{11} & 0 \\ 0 & 0 & 0 \end{pmatrix}, \qquad (2.12)$$

with $B_{11} = E_\perp h^2 (E_\parallel / E_\perp - 1)/4P$, where $E_\parallel$ and $E_\perp$ are the Young moduli in the parallel and transverse directions of the fibre and P is the number of layers of the laminate. Antisymmetric angle-ply laminates, on the other hand, have laminae oriented as same angle θ with respect to the laminate coordinate axis on the one

side of the middle-surface and the corresponding equal thickness laminae oriented at $-\theta$ on the other side at the same distance form the middle-surface. In this case,

$$\mathbf{B} = \begin{pmatrix} 0 & 0 & B_{16} \\ 0 & 0 & B_{26} \\ B_{16} & B_{26} & 0 \end{pmatrix}. \qquad (2.13)$$

General asymmetric laminates obtained by the asymmetric stacking of isotropic layers with different material properties about the middle-surface have finally

$$\mathbf{B} = \begin{pmatrix} B_{11} & B_{12} & 0 \\ B_{12} & B_{22} & 0 \\ 0 & 0 & B_{66} \end{pmatrix}. \qquad (2.14)$$

In §2c, we start with a focus on the case of orthotropic strips for which $B_{ij} = 0$, while the case of angle-ply laminates is discussed in §4 in the context of tristable strips.

(c) Equilibrium conformations

In the case of naturally flat strips with no coupling between stretching and bending (i.e. $B_{ij} = 0$ and $\delta_{ij} = D_{ij}$), equation (2.10) reduces to the equation given by Reissner (1992) for the case of an inhomogeneous anisotropic strip,

$$\alpha_{22}\frac{\partial^4 M_x}{\partial x^4} + \frac{\kappa_y}{D_{11}} M_x = \kappa_y \frac{D_{12}\kappa_y^2 + D_{16}\kappa_y\kappa_{xy} + D_{11}\kappa_{xy}^2}{D_{11}}.$$

Now, letting

$$\varphi_1 = -\frac{\beta_{21}\kappa_y}{\alpha_{22}\delta_{11} + \beta_{21}^2}, \qquad \varphi_2 = \frac{\kappa_y^2}{\alpha_{22}\delta_{11} + \beta_{21}^2}$$

and

$$\varphi_3 = \frac{\kappa_y\{\delta_{11}(c_x c_y - c_{xy}^2 + \kappa_{xy}^2) + \kappa_y[\delta_{12}(\kappa_y - c_y) + \delta_{16}(\kappa_{xy} - c_{xy}) - \delta_{11}c_x]\}}{\alpha_{22}\delta_{11} + \beta_{21}^2},$$

the solution of equation (2.10) that satisfies the homogeneous boundary conditions (2.11) is given by

$$M_x = -\delta_{11}(\kappa - \kappa_0) + \delta_{11}C_1\cosh k_1 x \cos k_2 x + \delta_{11}C_2\sinh k_1 x \sin k_2 x, \qquad (2.15)$$

where

$$\kappa_0 = \frac{(c_x c_y - c_{xy}^2) + \kappa_{xy}^2}{\kappa_y} \qquad (2.16a)$$

and

$$\kappa = c_x + \frac{\delta_{12}}{\delta_{11}}(c_y - \kappa_y) + \frac{\delta_{16}}{\delta_{11}}(c_{xy} - \kappa_{xy}); \qquad (2.16b)$$

$$C_1 = (\kappa - \kappa_0)\left(\frac{k_1\cosh ak_1 \sin ak_2 + k_2\sinh ak_1 \cos ak_2}{k_1\sin ak_2 \cos ak_2 + k_2\sinh ak_1 \cosh ak_1}\right) \qquad (2.17a)$$

and

$$C_2 = (\kappa - \kappa_0)\left(\frac{k_2\cosh ak_1 \sin ak_2 - k_1\sinh ak_1 \cos ak_2}{k_1\sin ak_2 \cos ak_2 + k_2\sinh ak_1 \cosh ak_1}\right), \qquad (2.17b)$$

with

$$k_1 = \left(\frac{\sqrt{\varphi_2} + \varphi_1}{2} \right)^{1/2} \quad \text{and} \quad k_2 = \left(\frac{\sqrt{\varphi_2} - \varphi_1}{2} \right)^{1/2}.$$

The longitudinal stress N_y and the transverse curvature κ_x can be readily calculated by replacing M_x in equations (2.7b) and (2.9a). This yields

$$N_y = \delta_{11} C_2' \cosh k_1 x \cos k_2 x - \delta_{11} C_1' \sinh k_1 x \sin k_2 x, \tag{2.18}$$

with

$$C_1' = \frac{(\alpha_{22}\delta_{11})^{1/2} C_1 + \beta_{21} C_2}{\alpha_{22}\delta_{11} + \beta_{21}^2} \quad \text{and} \quad C_2' = \frac{(\alpha_{22}\delta_{11})^{1/2} C_2 - \beta_{21} C_1}{\alpha_{22}\delta_{11} + \beta_{21}^2},$$

and finally

$$\kappa_x = \kappa_0 + (C_1 + \beta_{21} C_2') \cosh k_1 x \cos k_2 x + (C_2 - \beta_{21} C_1') \sinh k_1 x \sin k_2 x. \tag{2.19}$$

Equation (2.19) is equivalent to an expression given by Galletly & Guest (2004b) for the case of a bistable composite slit tube. We will now examine the effect of spontaneous curvature and elastic anisotropy on the energy landscape of elastic strips.

3. Multi-stable configurations of orthotropic strips

As a starting point in our analysis, we consider the case of orthotropic strips. For this class of materials, there is no coupling between stretching and bending; hence $B_{ij} = 0$, and the $\mathbf{A}$ and $\mathbf{D}$ matrices can be expressed in the following form:

$$\mathbf{A} = tE_0 \begin{bmatrix} 1 & \nu & 0 \\ \nu & \beta & 0 \\ 0 & 0 & \rho\left(1 - \frac{\nu^2}{\beta}\right) \end{bmatrix} \quad \text{and} \quad \mathbf{D} = \frac{t^3 E_0}{12} \begin{bmatrix} 1 & \nu & 0 \\ \nu & \beta & 0 \\ 0 & 0 & \rho\left(1 - \frac{\nu^2}{\beta}\right) \end{bmatrix},$$

where $E_0 = E/(1 - \nu^2/\beta)$ and, following Seffen (2007), we have called

$$E_x = E, \quad E_y = \beta E, \quad G = \rho E, \quad \nu_{yx} = \nu \quad \text{and} \quad \nu_{xy} = \frac{\nu}{\beta},$$

where E_x and E_y are the Young moduli in the x and y directions, G is the shear modulus, and ν_{xy} and ν_{yx} are the Poisson ratios. The conditions for the matrices $\mathbf{A}$ and $\mathbf{D}$ to be positive definite translate into the requirement $\beta > \nu^2$ and $\rho > 0$ (Vidoli & Maurini 2009). The transverse curvature (2.19) and the longitudinal stress (2.18) then simplify to yield

$$\kappa_x = \kappa_0 + C_1 \cosh kx \cos kx + C_2 \sinh kx \sin kx \tag{3.1a}$$

and

$$N_y = (t\beta ED)^{1/2} (C_2 \cosh kx \cos kx - C_1 \sinh kx \sin kx), \tag{3.1b}$$

where $D = t^3 E/12(1 - \nu^2/\beta)$, $k_1 = k_2 = k$ and

$$k = \left(\frac{t\beta E}{4D} \kappa_y^2 \right)^{1/4}.$$

The stretching energy density u_s and the bending energy density u_b are obtained by substituting (3.1) into (2.5) and yield

$$u_s = \frac{1}{2t\beta E} N_y^2 \tag{3.2a}$$

and

$$u_b = \tfrac{1}{2} D \left[\chi_x^2 + \beta \chi_y^2 + 2\nu \chi_x \chi_y + \rho \left(1 - \frac{\nu^2}{\beta} \right) \chi_{xy}^2 \right]. \tag{3.2b}$$

Integrating (3.2) along the width of the strips, we obtain the total stretching energy per unit length

$$u_s = \frac{1}{2} D (\kappa - \kappa_0)^2 \left(\frac{\Psi}{2k} - 2a\Phi \right), \tag{3.3}$$

where

$$\Psi = \frac{\cosh 2ka - \cos 2ka}{\sinh 2ka + \sin 2ka} \quad \text{and} \quad \Phi = \frac{\sinh 2ka \sin 2ka}{(\sinh 2ka + \sin 2ka)^2},$$

and the bending energy

$$u_b = aD \Bigg[(\kappa_0 - c_x)^2 + \beta (\kappa_y - c_y)^2 + 2\nu (\kappa_0 - c_x)(\kappa_y - c_y)$$

$$+ \rho \left(1 - \frac{\nu^2}{\beta} \right) (\kappa_{xy} - c_{xy})^2 + \frac{\eta}{2ka} (\kappa - \kappa_0)\Psi + (\kappa - \kappa_0)^2 \Phi \Bigg], \tag{3.4}$$

where

$$\eta = \frac{5}{2\kappa_y} [(\kappa_y - c_y)(\nu \kappa_y - c_x) + (\kappa_{xy}^2 - c_{xy}^2)]. \tag{3.5}$$

Before proceeding with the analysis, it is useful to introduce a set of dimensionless quantities defined by

$$\hat{x} = \frac{x}{a}, \quad \hat{t} = \frac{t}{a}, \quad \hat{c}_i = ac_i \quad \text{and} \quad \hat{\kappa}_i = a\kappa_i \quad (i = x, y, xy),$$

so that the dimensionless stresses and energies per unit length are given by

$$\hat{N}_y = \frac{N_y}{aE}, \quad \hat{U}_s = \frac{u_s}{taE}, \quad \hat{U}_b = \frac{u_b}{taE} \quad \text{and} \quad \hat{U} = \hat{U}_s + \hat{U}_b.$$

$\hat{U}$ is thus the total elastic energy of a strip that accounts for both stretching and bending. In the following sections, we will analyse the 'energy landscape' embodied in $\hat{U}$ and given by (3.3) and (3.4) in a variety of scenarios. We will start by considering configurations of constant transverse curvature $\hat{\kappa}_x$ and then move on to the more general case in which $\hat{\kappa}_x$ is allowed to vary across the strip. In §3c, we will examine the limit of vanishing bending stiffness and show how tristability arises in this setting for a broad range of spontaneous curvatures.

(a) Uniform curvature configurations

To understand the energy landscape of the strip, we analyse the total elastic energy $\hat{U}$ given by (3.3) and (3.4). We first focus on configurations having constant

transverse curvature $\hat{\kappa}_x$: if $\hat{\kappa}_y$ is non-zero; from equations (2.17) and (3.1a), it follows that $C_1 = C_2 = 0$ and $\hat{\kappa} = \hat{\kappa}_0$. This solution has zero longitudinal stress and, as a consequence, is an isometry of the base configuration: a deformation that preserves the local metric of the shell so that $\boldsymbol{\epsilon} = \mathbf{0}$. The latter statement can be also verified by calculating the Gaussian curvature of the deformed strip. Because $\hat{\kappa}_x = \hat{\kappa} = \hat{\kappa}_0$, equation (2.16$a$) yields

$$\hat{\kappa}_x = \frac{(\hat{c}_x \hat{c}_y - \hat{c}_{xy}^2) + \hat{\kappa}_{xy}^2}{\hat{\kappa}_y}, \tag{3.6}$$

which implies that $\hat{\kappa}_x \hat{\kappa}_y - \hat{\kappa}_{xy}^2 = \hat{c}_x \hat{c}_y - \hat{c}_{xy}^2$ as required by Gauss' *theorema egregium* (Kreyszig 1991). The corresponding total elastic energy per unit length $\hat{U}$ is given by

$$\hat{U} = \frac{\hat{t}^2}{12}[\beta(\hat{\kappa}_y - \hat{c}_y)^2 + \rho(\hat{\kappa}_{xy} - \hat{c}_{xy})^2]. \tag{3.7}$$

The condition $\hat{\kappa} = \hat{\kappa}_0$ used to obtain the isometric solution (3.6) describes, in the plane $(\hat{\kappa}_y, \hat{\kappa}_{xy})$, a continuous set of configurations of zero stretching energy. The explicit form of this geometrical locus is given by

$$\nu \hat{\kappa}_y^2 + \hat{\kappa}_{xy}^2 - (\hat{c}_x + \nu \hat{c}_y)\hat{\kappa}_y = \hat{c}_{xy}^2 - \hat{c}_x \hat{c}_y, \tag{3.8}$$

which corresponds to an ellipse with focii at

$$\hat{\kappa}_{y,0} = \frac{1}{2\nu}(\hat{c}_x + \nu \hat{c}_y) \quad \text{and} \quad \hat{\kappa}_{xy,0} = 0,$$

and semi-axes $a_y = 1/\ell\sqrt{\nu}$ and $a_{xy} = 1/\ell$, with $\ell^{-2} = (1/4\nu)(\hat{c}_x - \nu \hat{c}_y)^2 + \hat{c}_{xy}^2$. The bending energy, however, suppresses this soft mode by selecting a minimum in this class of isometric deformations: the base configuration having $\hat{\kappa}_y = \hat{c}_y$ and $\hat{\kappa}_{xy} = \hat{c}_{xy}$.

A special but not necessarily isometric solution with constant curvature can be found by taking the limit $\hat{\kappa}_y \to 0$ of equation (3.1a), which gives

$$\hat{\kappa}_x = \hat{c}_x + \nu \hat{c}_y. \tag{3.9}$$

The corresponding longitudinal stress is given then by

$$\hat{N}_y = \frac{\hat{t}}{6}\beta(3\hat{x}^2 - 1)[(\hat{c}_x \hat{c}_y - \hat{c}_{xy}^2) + \hat{\kappa}_{xy}^2], \tag{3.10}$$

using which we can calculate the total elastic energy as

$$\hat{U} = \beta \left\{ \frac{1}{45}[(\hat{c}_x \hat{c}_y - \hat{c}_{xy}^2) + \hat{\kappa}_{xy}^2]^2 + \frac{\hat{t}^2}{12}\left[\hat{c}_y^2 + \frac{\rho}{\beta}(\hat{\kappa}_{xy} - \hat{c}_{xy})^2 \right] \right\}. \tag{3.11}$$

This class of deformations belongs to the set of isometries only when the first term on the left-hand side of equation (3.11) vanishes, namely when

$$\hat{\kappa}_{xy}^2 = \hat{c}_{xy}^2 - \hat{c}_x \hat{c}_y = -\hat{K}_0. \tag{3.12}$$
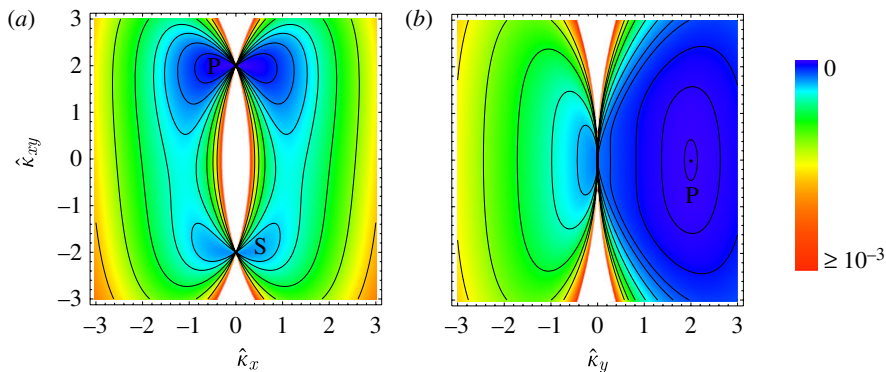
Figure 2. Contour plot of the total elastic energy per unit length $\hat{U}$ from (3.3) and (3.4) in the plane $(\hat{\kappa}_y, \hat{\kappa}_{xy})$. The labels P and S indicate the primary and secondary minima. (*a*) $\hat{c}_x = \hat{c}_y = 0$ and $\hat{c}_{xy} = 2$. The strip has a secondary minimum at $\hat{\kappa}_{xy} \approx -\hat{c}_{xy}$. (*b*) $\hat{c}_x = \hat{c}_{xy} = 0$ and $\hat{c}_y = 2$. The strip has a single equilibrium configuration. The other relevant parameters are $\beta = 10$, $\rho = 1$, $\nu = 1/3$ and $\hat{t} = 10^{-2}$. (Online version in colour.)

Clearly, this is possible only when the initial Gaussian curvature $\hat{K}_0$ is negative or zero. In the latter case, the strip has only one minimum corresponding to the base configuration (figure 2*b*).

However, a secondary equilibrium configuration of constant curvature is obtained if $\hat{c}_x = \hat{c}_y = 0$ and $\hat{c}_{xy} \neq 0$, when equation (3.11) reads

$$\hat{U} = \beta \left\{ \frac{1}{45}(\hat{\kappa}_{xy}^2 - \hat{c}_{xy}^2)^2 + \frac{\hat{t}^2}{12}\frac{\rho}{\beta}(\hat{\kappa}_{xy} - \hat{c}_{xy})^2) \right\}. \tag{3.13}$$

Then, in addition to the base configuration $\hat{\kappa}_{xy} = \hat{c}_{xy}$, the energy has a secondary minimum corresponding to the twisting curvature

$$\hat{\kappa}_{xy} = -\frac{1}{2}\left\{ \hat{c}_{xy} + \sqrt{\hat{c}_{xy}^2 - \frac{15}{2}\left(\frac{\rho}{\beta}\right)\hat{t}^2} \right\}, \tag{3.14}$$

which is approximately $\hat{\kappa}_{xy} \approx -\hat{c}_{xy}$ (figure 2*a*). The stability of the secondary minimum depends on ρ and β, as well as the Poisson ratio ν. To assess this, we calculate the components of the Hessian matrix,

$$\frac{\partial^2 \hat{U}}{\partial \hat{\kappa}_y^2} = \beta \left\{ \frac{\hat{t}^2}{6} + \frac{4}{45}\nu (\hat{\kappa}_{xy}^2 - \hat{c}_{xy}^2) + \frac{16}{945}\frac{(\nu^2 - \beta)}{\hat{t}^2}(\hat{\kappa}_{xy}^2 - \hat{c}_{xy}^2)^2 \right\},$$

$$\frac{\partial^2 \hat{U}}{\partial \hat{\kappa}_y \partial \hat{\kappa}_{xy}} = 0 \quad \text{and} \quad \frac{\partial^2 \hat{U}}{\partial \hat{\kappa}_{xy}^2} = -\frac{4}{45}\beta(\hat{c}_{xy}^2 - 3\kappa_{xy}^2) + \frac{\hat{t}^2}{6}\rho,$$

where $\hat{\kappa}_{xy}$ is given by equation (3.14). In order for the secondary minimum to be stable, the eigenvalues of the Hessian matrix must be positive. Upon expanding

$\partial^2 \hat{U}/\partial \hat{\kappa}_y^2$ at the second order in $\hat{t}$, this condition reduces to the following inequality:

$$\beta - 2\nu\rho - \frac{10}{7}\left(1 - \frac{\nu^2}{\beta}\right)\rho^2 > 0.$$

This implies the following requirement on ρ:

$$\rho < \frac{\beta}{\nu + \sqrt{(10\beta - 3\nu^2)/7}}. \tag{3.15}$$

In summary, strips having zero spontaneous principal curvatures $\hat{c}_x = \hat{c}_y = 0$ and non-zero spontaneous twist $\hat{c}_{xy}$ admit a secondary equilibrium configuration where the principal curvatures vanish, i.e. $\hat{\kappa}_x = \hat{\kappa}_y = 0$, while the twisting curvature is reversed $\hat{\kappa}_{xy} \approx -\hat{c}_{xy}$. The secondary minimum is stable for low enough shear modulus, a scenario previously discussed by Seffen (2007) for the case of an elliptical plate endowed with pure twist. The most important difference between the two cases is that here the strip has zero bending moment along the lateral edges, unlike the plate investigated by Seffen, which can support a finite bending moment at the boundary. As a consequence, the transverse curvature $\hat{\kappa}_x$, which is a free parameter in uniform curvature models, is here adjusted in order to maintain the boundary moment-free, and this severely restricts the space of possible uniform curvature configurations.

The previous situation is an example of bistability in a strip with a negative spontaneous Gaussian curvature $\hat{K}_0 = -\hat{c}_{xy}^2$, where the principal curvatures $\hat{c}_x$ and $\hat{c}_y$ vanish identically, while the surface is purely twisted. However, when $\hat{c}_x \hat{c}_y \neq 0$ and $\hat{K}_0 < 0$, the strip also exhibits a secondary equilibrium configuration, albeit with a variable transverse curvature $\hat{\kappa}_x$ discussed in §3b.

(b) Non-uniform curvature configurations

When the constraint of constant curvature is lifted, new minima appear in the energy landscape. Figure 3 shows a contour plot of the total elastic energy in the plane $(\hat{\kappa}_x, \hat{\kappa}_{xy})$ for the two cases $\hat{c}_x \hat{c}_y > 0$ (figure 3a), $\hat{c}_x \hat{c}_y < 0$ (figure 3b) and $\hat{c}_{xy} = 0$ in both cases. For positive spontaneous Gaussian curvatures, the energy minima are those described in §3b, when $\hat{\kappa}_{xy} = 0$. The transverse curvature $\hat{\kappa}_x$ associated with the secondary minimum at $\hat{\kappa}_y < 0$ is mostly constant across the width of the strip and equal to

$$\hat{\kappa}_0 = \frac{(\hat{c}_x \hat{c}_y - \hat{c}_{xy}^2) + \hat{\kappa}_{xy}^2}{\hat{\kappa}_y},$$

with exception for a boundary layer (figure 4). This phenomenon, first noted by Lamb (1891), is due to the rapid build-up of the bending moment M_x from zero at the edges to a non-zero value that inevitably develops in any configuration other than the base state (see Mansfield 1989 for a detailed explanation). An estimate of the size of the boundary layer is given by $1/k \approx (t/|\kappa_y|)^{1/2}$; however, it vanishes in a strip of lenticular cross section whose thickness (hence the bending moment) smoothly tapers and vanishes at the edges.
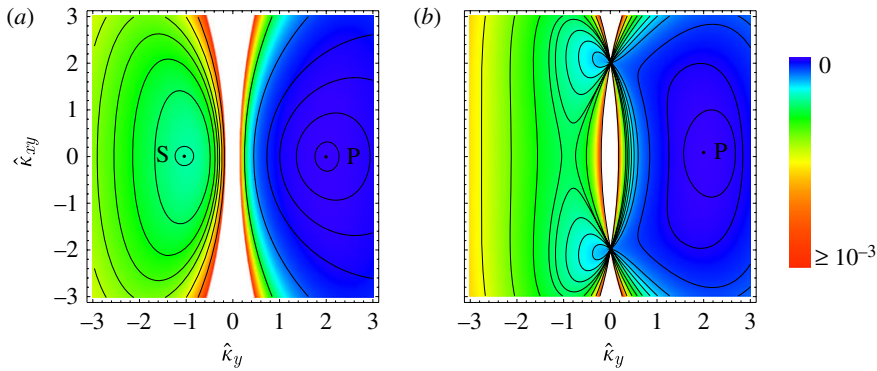
Figure 3. Contour plot of the total elastic energy per unit length $\hat{U}$ from (3.3) and (3.4) in the plane $(\hat{\kappa}_y, \hat{\kappa}_{xy})$. The labels P and S indicate the primary and secondary minima. (a) $\hat{c}_x = \hat{c}_y = 2$ and $\hat{c}_{xy} = 0$. In addition to the base configuration, the strip has a second equilibrium at $\hat{\kappa}_y \approx -(\hat{c}_x \hat{c}_y)^{1/2}$. (b) $\hat{c}_x = -2$, $\hat{c}_y = 2$ and $\hat{c}_{xy} = 0$. In this case, the strip has only one equilibrium configuration. Note that the region $\hat{\kappa}_y < 0$ in the previous example was separated from the region $\hat{\kappa}_y > 0$ by an energy barrier of height $\hat{U}_0 \sim \hat{K}_0^2$ is now connected by two 'passes' located at $\hat{\kappa}_{xy}^2 = \pm(\hat{c}_x \hat{c}_y)^{1/2}$. The other relevant parameters are $\beta = 10$, $\rho = 1$, $\nu = 1/3$ and $\hat{t} = 10^{-2}$. (Online version in colour.)
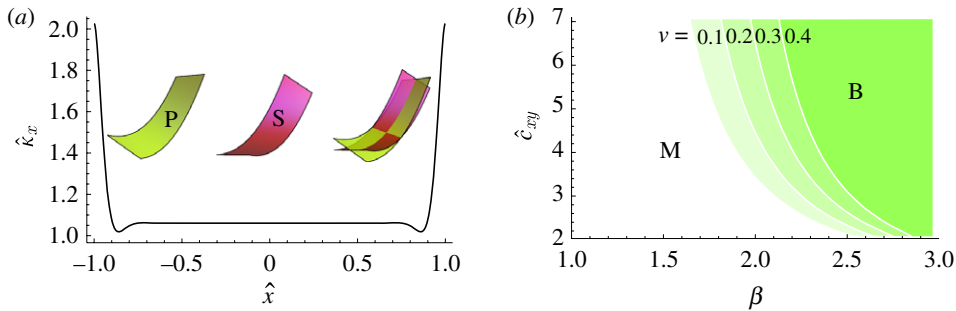

Figure 4. (a) The dimensionless transverse curvature $\hat{\kappa}_x$ associated with the secondary equilibrium configuration of a strip with spontaneous positive Gaussian curvature as a function of the dimensionless distance $\hat{x}$ from the centreline. The relevant parameters are $\hat{c}_x = 2$, $\hat{c}_y = 1$, $\hat{c}_{xy} = 0$, $\beta = 10$, $\rho = 1$ and $\hat{t} = 10^{-2}$. The transverse curvature is constant and equal to κ_0, with exception for a boundary layer. In the inset, a schematic of the primary (P) and secondary (S) equilibria is shown. (b) Monostability/bistability (M/B) phase diagram in the plane $(\beta, \hat{c}_{xy})$ for a strip of negative Gaussian curvature and different values of the Poisson ratio ν. The spontaneous principal curvatures are $\hat{c}_x = 2$ and $\hat{c}_y = 1$. The other relevant parameters are $\rho = 1$ and $\hat{t} = 10^{-2}$. (Online version in colour.)

On the other hand, for negative Gaussian curvature $\hat{c}_x \hat{c}_y < 0$ and $\hat{c}_{xy} = 0$, the secondary minimum becomes a saddle point and the elastic energy has only one minimum corresponding to the base configuration. It is interesting to notice, in this latter case, that the regions of positive and negative $\hat{\kappa}_y$ of the energy landscape are separated by a barrier of height $\hat{U}(\hat{\kappa}_y = 0) \sim \hat{K}_0^2$ that is large everywhere with exception for two 'passes' at $\hat{\kappa}_{xy} = \pm(-\hat{c}_x \hat{c}_y)^{1/2}$ (figure 5). The existence of these passes along the energy barrier at $\hat{\kappa}_y = 0$ is the reason for the non-existence of a secondary equilibrium configuration in strips with
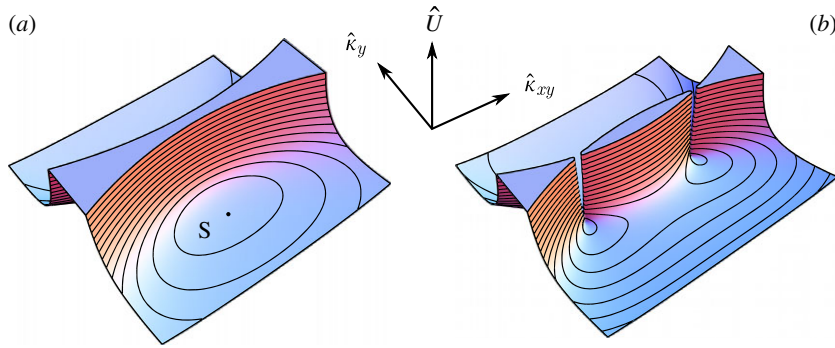
Figure 5. The elastic energy given by (3.3) and (3.4) as function of $\hat{\kappa}_y$ and $\hat{\kappa}_{xy}$ for a strip of spontaneous positive Gaussian curvature ((a) $\hat{c}_x = \hat{c}_y = 1$) and a strip of spontaneous negative Gaussian curvature ((b) $\hat{c}_x = -\hat{c}_y = 0$). In the former, the $\hat{\kappa}_y < 0$ portion of the energy landscape is separated from the $\hat{\kappa}_y > 0$ region by a large energy barrier of height $\hat{U}(\hat{\kappa}_y = 0) \sim \hat{K}_0^2$. This implies the existence of a secondary minimum (labelled S). In the case of strips of negative spontaneous Gaussian curvature, on the other hand, the energy barrier has two passes at $\hat{\kappa}_y = 0$ and $\hat{\kappa}_{xy} = \pm(-\hat{K}_0)^{1/2}$, and the secondary minimum is replaced by a saddle point. The flat plateau in the energy barriers is a graphical artefact owing to the limited range of $\hat{U}$ shown. (Online version in colour.)

spontaneous negative Gaussian curvature. As explained in §3a and summarized in equation (3.12), the stretching energy associated with the barrier at $\hat{\kappa}_y = 0$ scales like $\hat{U}_s \sim (\hat{K}_0 + \hat{\kappa}_{xy}^2)^2$ and, in the presence of spontaneous *negative* Gaussian curvature, it can be relieved through twist. This leads to the formation of passes at $\hat{\kappa}_{xy} = \pm(-\hat{K}_0)^{1/2}$, shown in figures 3 and 5, which allow the transverse curvature $\hat{\kappa}_y$ to be switched from positive to negative (and vice versa) *isometrically*. Positive spontaneous Gaussian curvatures, on the other hand, cannot be accommodated through twist and thus there are no passages across the energy barrier at $\hat{\kappa}_y = 0$; consequently, there is a secondary minimum.

To get an intuitive sense of these passes in the energy landscape, imagine a strip of positive spontaneous Gaussian curvature (figure 6a). To evert the strip, one choice is to flatten the strip and then reverse its curvature. Because the strip is naturally curved, the intermediate flat conformation will suffer a large strain, and this corresponds to the large energy barrier shown in figure 5. On the other hand, if the strip is naturally shaped like a saddle (figure 6b), turning the strip inside-out can be achieved by pulling apart two opposite corners until the strip is fully extended and maximally twisted, and then bend it into the new configuration. The latter deformation can be performed without stretching the surface and thus with no energy cost other than bending, in contrast with the case of a strip with positive $\hat{K}_0$. Similar deformation pathways have been analysed by Fernandes *et al.* (2010) as possible strategies to achieve shape control of bistable composite plates using embedded actuators.

However, when strips with negative spontaneous Gaussian curvature $\hat{K}_0 < 0$ have a non-zero spontaneous twist $\hat{c}_{xy}$, they admit bistable configurations. In addition to the configuration with constant curvature described in §3a in the special case $\hat{c}_x = \hat{c}_y = 0$ and $\hat{c}_{xy} \neq 0$, another configuration can be obtained by
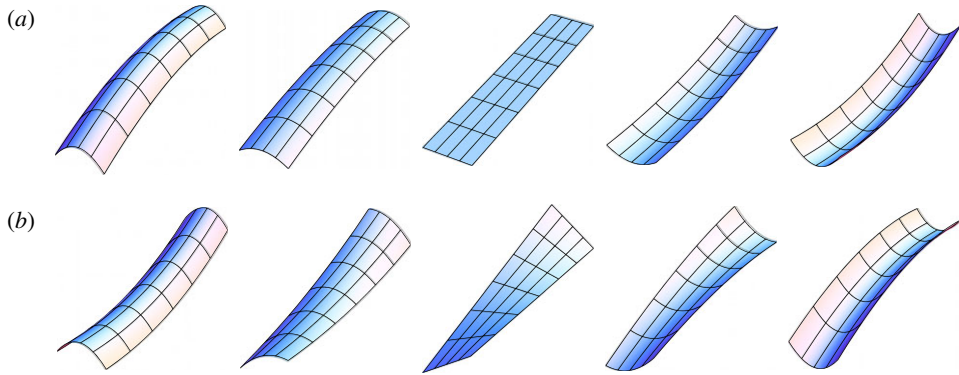
(a)

(b)

Figure 6. Sequence of deformations of a strip of spontaneous (*a*) positive and (*b*) negative Gaussian curvature associated with curvature reversal. While the former sequence requires the strip to become temporarily flat and thus produces large strains, the latter can be performed isometrically at zero stretching energy cost. The existence of this low-energy deformation in strips of spontaneous negative curvature is responsible for the formation of the passes shown in figure 5, hence the lack of a secondary minimum. (Online version in colour.)
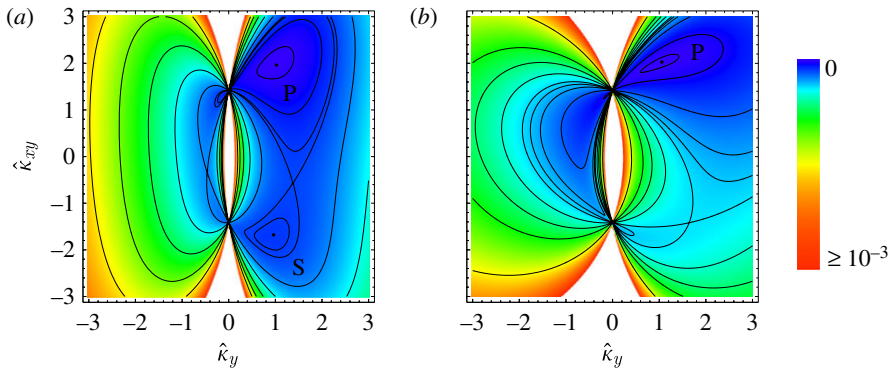

Figure 7. Contour plot of the total elastic energy per unit length $\hat{U}$ from (3.3) and (3.4) in the plane $(\hat{\kappa}_y, \hat{\kappa}_{xy})$. The labels P and S indicate the primary and secondary minima. In both plots, the spontaneous curvatures are set at $\hat{c}_x = 2$, $\hat{c}_y = 1$ and $\hat{c}_{xy} = 2$. (*a*) The case $\beta = 10$, in addition to the base configuration, the strip as a secondary minimum in proximity of the point $(\hat{\kappa}_y, \hat{\kappa}_{xy}) = (\hat{c}_y, -\hat{c}_{xy})$. Such a minimum disappears when $\beta = 1$ (*b*). The other relevant parameters are $\rho = 1$, $\nu = 1/3$ and $\hat{t} = 10^{-2}$. (Online version in colour.)

setting $\hat{c}_x \hat{c}_y \neq 0$ with $\hat{K}_0 < 0$. Figure 7 shows a contour plot of the total elastic energy (3.3) and (3.4) of a strip with $\hat{c}_x = 2$, $\hat{c}_y = 1$ and $\hat{c}_{xy} = 2$, thus $\hat{K}_0 = -2$. Figure 7*a* (in which $\beta = 10$) shows a secondary minimum in the proximity of the point $(\hat{\kappa}_y, \hat{\kappa}_{xy}) = (\hat{c}_y, -\hat{c}_{xy})$. When the anisotropy parameter β is decreased, however, the secondary minimum disappears and the energy landscape is again characterized by a unique minimum corresponding to the base configuration.

Such a configuration has energy $\hat{U} \approx (\rho/\beta)\hat{c}_{xy}^2$, and has a minimum for large values of β/ρ. One might expect that the value of β/ρ necessary to have a secondary minimum of this kind would increase monotonically with $\hat{c}_{xy}$;

however, this is incorrect. In figure 4, we show the 'phase diagram' of the monostability/bistability region for a strip with spontaneous curvatures $\hat{c}_x = 2$ and $\hat{c}_y = 1$ in the plane $(\beta/\rho, \hat{c}_{xy})$. Upon fixing the spontaneous twist $\hat{c}_{xy}$, the bistability region can be accessed by increasing β/ρ, as expected. However, for fixed β/ρ, the bistable region is accessed by increasing the spontaneous twist. The origin of this behaviour is related to the height of the energy barrier at $\hat{\kappa}_y = 0$ separating the secondary minimum from the basin of attraction of the base configuration at $\hat{\kappa}_y < 0$. From equation (3.11), we see that the height of such a barrier $\hat{U} \approx \beta \hat{K}_0^2$. For fixed β/ρ, decreasing $\hat{c}_{xy}$ (or equivalently $|\hat{K}_0|$) will lower the height of the barrier until the basin of attraction associated with the portion where $\hat{\kappa}_y < 0$ of the base configuration will merge with that of the secondary minimum. For values of $\hat{c}_{xy}$ smaller than this critical value, the energy landscape is then characterized by a unique minimum (i.e. the base configuration) surrounded by a large C-shaped basin of attraction that starts from the base configuration and extends in the region $\hat{\kappa}_y < 0$ penetrating the barrier at $\hat{\kappa}_y = 0$ through the passes located at $\hat{\kappa}_{xy} = \pm(-\hat{K}_0)^{1/2}$ (figure 7b). Once again, the presence of two regions across the barrier at $\hat{\kappa}_y = 0$ where the stretching energy drops, plays a crucial role in assuring the existence of bistable configurations.

In summary, orthotropic strips exhibit various forms of bistability depending on their spontaneous curvature and elastic moduli. The simplest bistable configurations have constant curvature throughout the width of the strip and correspond to isometries of the base configuration. Non-isometric secondary equilibria have, on the other hand, variable transverse curvature $\hat{\kappa}_x$; this is approximately constant and equal to $\hat{\kappa}_0 = (\hat{K}_0 + \hat{\kappa}_{xy}^2)/\hat{\kappa}_y$ in the bulk of the strip, but abruptly jumps to $\hat{\kappa} = \hat{c}_x + \nu(\hat{c}_y - \hat{\kappa}_x)$ near the edges to relieve the bending moment that forms in the bulk when the strip is in a configuration different from the base one. For strips with positive spontaneous Gaussian curvature, in particular, the secondary equilibrium configuration has transverse curvature of opposite sign relative to the base configuration. Strips with negative spontaneous Gaussian curvature, on the other hand, do not possess a secondary equilibrium configuration unless they have sufficient spontaneous twist $\hat{c}_{xy}$. The existence of bistability in this case also relies on the value of the ratio β/ρ between the Young modulus along the longitudinal direction and the shear modulus. Figure 8 shows a phase diagram of the monostability/bistability regions in the plane $(\hat{c}_x, \hat{c}_y)$ for strips of various spontaneous twist $\hat{c}_{xy}$.

(c) Tristable configurations

As we mentioned in the introduction of §3, the requirement for the matrices **A** and **D** to be positive definite translates into the conditions $\beta > \nu^2$ and $\rho > 0$. In this section, we show that when the limit $\beta \to \nu^2$ is approached, a new stable minimum appears in the energy landscape of the configurations allowing for *tristability*. The presence of three minima in the reduced quasi-one-dimensional geometry of elastic strips complements the appearance of such a landscape for corrugated strips, where tristability arises as a consequence of the coupling between internal prestresses created while imprinting the corrugation and nonlinear geometrical changes during deformation (Norman *et al.* 2008).
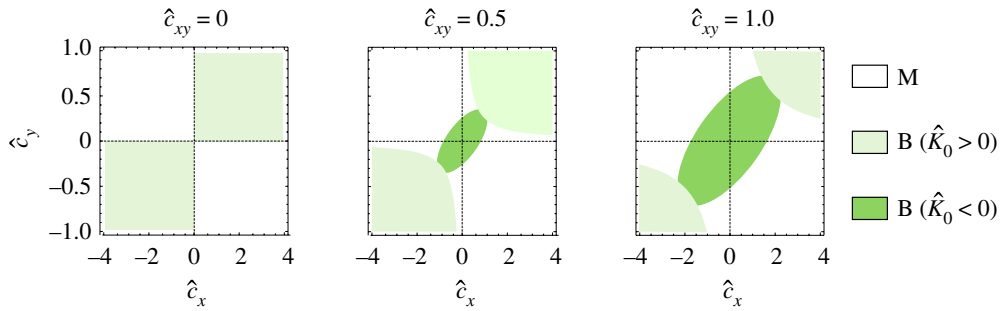
Figure 8. Phase diagram of the monostability (M, in white) and bistability region (B, light shaded, $\hat{K}_0 > 0$; dark shaded, $\hat{K}_0 < 0$) in the plane $(\hat{c}_x, \hat{c}_y)$ for strips of various spontaneous twist $\hat{c}_{xy}$. Different shades correspond to positive (light) and negative (dark) spontaneous Gaussian curvature. For zero spontaneous twist, the bistable configuration exists only in the region of positive Gaussian curvature. For $\hat{c}_{xy} \neq 0$, on the other hand, bistability also occurs in a range of negative Gaussian curvature. The relevant parameters are $\beta = 10$, $\rho = 1$, $\nu = 1/3$ and $\hat{t} = 10^{-2}$. (Online version in colour.)

Letting $\beta = \nu^2 + \epsilon$ and expanding equations (3.3) and (3.4) in powers of ϵ gives

$$\hat{U} = \nu^2 \left\{ \frac{1}{45} \left[(\hat{\kappa}_y - \hat{c}_y)(\nu\hat{\kappa}_y - \hat{c}_x) + \hat{\kappa}_{xy}^2 - \hat{c}_{xy}^2 \right]^2 \right.$$

$$\left. + \frac{1}{12}\hat{t}^2 \left[(\hat{\kappa}_y - \hat{c}_y)^2 + \frac{\rho}{\nu^2}(\hat{\kappa}_{xy}^2 - \hat{c}_{xy}^2) \right] \right\} + o(\epsilon). \tag{3.16}$$

Then, with $\hat{\kappa}_{xy} = \hat{c}_{xy}$, it is easy to prove that $\partial \hat{U}/\partial\hat{\kappa}_y = 0$ when $\hat{\kappa}_y = \hat{c}_y$ and also when

$$\hat{\kappa}_y^{\pm} = \frac{1}{4}\left\{ \hat{c}_y + \frac{1}{\nu}\left[3\hat{c}_x \pm \sqrt{(\hat{c}_x - \nu\hat{c}_y)^2 - 30\,\hat{t}^2} \right] \right\}. \tag{3.17}$$

Thus, in addition to the base configuration and the secondary minimum at $\hat{\kappa}_y < 0$ discussed in §3b, the energy has a third minimum at $\hat{\kappa}_y = \hat{\kappa}_y^+$, while $\hat{\kappa}_y^-$ is the location of the maximum separating the third minimum from the base configuration. For relatively thin shells, $\hat{t} \ll 1$ so that one finds simply $\hat{\kappa}_y^+ \approx \hat{c}_x/\nu$ and $\hat{\kappa}_y^- \approx (\hat{c}_y + \hat{c}_x/\nu)/2$. The energy of the third minimum is given approximately by

$$\hat{U}(\hat{\kappa}_y^+) \approx \frac{1}{12}\hat{t}^2\nu^2\left(\hat{c}_y - \frac{\hat{c}_x}{\nu}\right)^2. \tag{3.18}$$

Figure 9 shows a contour plot of the total elastic energy per unit length $\hat{U}$ from (3.3) and (3.4) for $\hat{c}_x = 1$, $\hat{c}_y = 2$, $\hat{c}_{xy} = 0$ and $\beta = \nu^2 + 10^{-2}$, with $\nu = 1/3$ and $\rho = 1$. The primary, secondary and tertiary minima are indicated by the letters P, S and T, respectively.

In the limit $\beta \to \nu^2$, tristability has been noted by Vidoli & Maurini (2009) in the case of plates with free boundaries and uniform curvature, although the physical origins of this phenomenon were not discussed. In our simple setting, consistent with the arguments in §3a, there is a continuous set of configurations of zero stretching energy corresponding to the isometries of the base state. In the
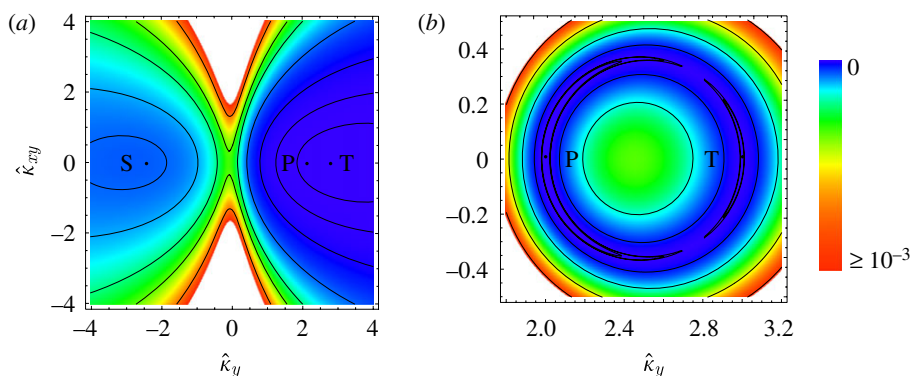
Figure 9. Contour plot of the total elastic energy per unit length $\hat{U}$ from (3.3) and (3.4) in the plane $(\hat{\kappa}_y, \hat{\kappa}_{xy})$ of a strip with $\beta = \nu^2 + 10^{-5}$ and spontaneous curvatures $\hat{c}_x = 1$, $\hat{c}_y = 2$ and $\hat{c}_{xy} = 0$. The primary, secondary and tertiary minima are indicated by the letters P, S and T, respectively. (*b*) Magnification of the region $\hat{\kappa}_y \in [1.8, 3.2]$, where the primary and tertiary minimum are located. The other relevant parameters are $\rho = 1$, $\nu = 1/3$ and $\hat{t} = 5 \times 10^{-4}$. (Online version in colour.)

plane $(\hat{\kappa}_y, \hat{\kappa}_{xy})$, this set describes an ellipse whose intersections with the $\hat{\kappa}_y$-axis (i.e. the untwisted configurations) are given by $\hat{\kappa}_y = \hat{c}_y$ and $\hat{\kappa}_y = \hat{c}_x/\nu$. The small but finite bending stiffness along the principal directions prevents this from being a true zero energy mode and instead leads to the existence of a soft mode by raising the energy of the minimum at $\hat{\kappa}_y = \hat{c}_x/\nu$; for $\beta \gg \nu^2$ (i.e. $D_{22} \gg D_{11}$), the minimum is completely suppressed. Taking the limit $\beta \to \nu^2$ corresponds to lowering the bending stiffness so that the energies of the two isometric configurations $\hat{\kappa}_y = \hat{c}_y$ and $\hat{\kappa}_y = \hat{c}_x/\nu$ are comparable again. This mechanism is completely general and independent of the specific geometry of the problem; any plate with shallow spontaneous curvature is amenable to a set of isometries, and multi-stability can in principle be obtained by setting $\det(\mathbf{D}) \sim 0$, which, in the case of orthotropic plates, corresponds in fact to $\beta \sim \nu^2$.

An interesting feature of this tristable energy landscape relies on the fact that the energy barrier separating the minima at $\hat{\kappa}_y = \hat{c}_y$ and $\hat{\kappa}_y = \hat{c}_x/\nu$ is generally much smaller than that located at $\hat{\kappa}_y = 0$ separating the base configuration with the minimum at $\hat{\kappa}_y < 0$. More precisely,

$$\hat{U}(\hat{\kappa}_y^-) \approx \frac{1}{720}(\hat{c}_x - \nu\hat{c}_y)^4. \tag{3.19}$$

while $\hat{U}(0) \approx (1/45)(\nu\hat{K}_0)^2$. Assuming $\hat{\kappa}_{xy} = \hat{c}_{xy} = 0$, the ratio between the height of these two energy barriers can be approximated as

$$\frac{\hat{U}(\hat{\kappa}_y^-)}{\hat{U}(0)} \approx \frac{1}{16}\left[\left(\frac{\hat{c}_x}{\nu\hat{c}_y}\right) + \left(\frac{\hat{c}_x}{\nu\hat{c}_y}\right)^{-1} - 2\right]^2 = \left[\sinh\frac{1}{2}\log\left(\frac{\hat{c}_x}{\nu\hat{c}_y}\right)\right]^4. \tag{3.20}$$

Assuming $\hat{c}_x < \hat{c}_y$, this ratio is $O(10^{-2})$. For $\hat{c}_x > \hat{c}_y$, the previous relation is no longer valid as the bending energy that was neglected to derive (3.20) becomes relevant; however, the order of magnitude of the ratio $\hat{U}(\hat{\kappa}_y^-)/\hat{U}(0)$ remains always of the order $O(10^{-2})$.
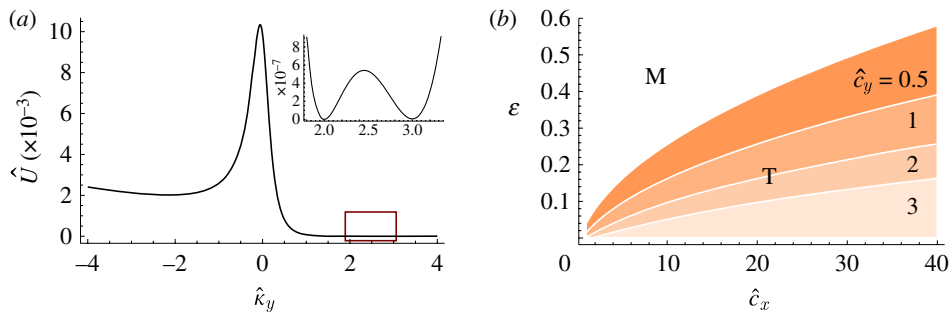
Figure 10. (*a*) Total elastic energy as a function of $\hat{\kappa}_y$ for a strip with $\beta - \nu^2 = 10^{-5}$ and spontaneous curvatures $\hat{c}_x = 1$, $\hat{c}_y = 2$ and $\hat{c}_{xy} = 0$. The inset shows a magnification of the boxed region $\hat{\kappa}_y \in [1.8, 3.3]$. The height of the barrier separating the base configuration from the tertiary minimum located at $\kappa_y^+ \approx c_x/\nu = 3$ is four orders of magnitude smaller than the barrier at $\hat{\kappa}_y = 0$. (*b*) Phase diagram in the plane $(\hat{c}_x, \epsilon = \beta - \nu^2)$ of the bistable (M, in white) and tristable (T, shaded) regions of a strip with zero spontaneous twist and various $\hat{c}_y$. The other relevant parameter are $\rho = 1$ and $\hat{t} = 10^{-2}$. (Online version in colour.)

The stability of the tertiary minimum at $\hat{\kappa}_y^+ \approx \hat{c}_x/\nu$ depends, in general, on the value of the Poisson ratio and the spontaneous curvatures $\hat{c}_x$ and $\hat{c}_y$. Figure 10 shows the bistability/tristability regions as a function of $\epsilon = \beta - \nu^2$ and $\hat{c}_x$ for various values of $\hat{c}_y$. Increasing the transverse spontaneous $\hat{c}_x$ allows tristability to occur at larger values of ϵ, thus further away from the limiting condition $\beta = \nu^2$.

4. Strips with coupling between stretching and bending

We now consider generally anisotropic strips, in which stretching and bending deformations are coupled through the **B** matrix, so that the total elastic energy density reads

$$u = \tfrac{1}{2}\{\alpha_{22}N_y^2 + \delta_{11}(\kappa_x - c_x)^2 + 2\delta_{12}(\kappa_x - c_x)(\kappa_y - c_y)$$
$$+ \delta_{22}(\kappa_y - c_y)^2 + \delta_{66}(\kappa_{xy} - c_{xy})^2\}, \tag{4.1}$$

where the elastic moduli α_{22} and δ_{ij} are given by (2.4), and N_y and κ_x have the general form given in equations (2.18) and (2.19). Because of the reduced dimensionality of this class of elastic objects, the coupling between stretching and bending is not expected to produce marked differences when compared with the case of orthotropic strips discussed in §3*c*, and indeed, for the majority of the choice of the elastic moduli α_{22} and δ_{ij}, the behaviour is qualitatively identical to that already described.

Under some circumstances, however, the finer control of the material properties characteristic of anisotropic laminates might be taken advantage of to enhance the region of tristability. To understand this possibility, we first note that the requirement for the matrices $\boldsymbol{\alpha}$ and $\boldsymbol{\delta}$ to be positive-definite, translates here into the condition $\alpha_{22} > 0$, $\delta_{66} > 0$ and $\delta_{11}\delta_{22} > \delta_{12}^2$. If the latter condition, in particular, is only weakly satisfied, the strip will be tristable for some value of the spontaneous curvatures c_x and c_y. To illustrate this point, let us consider the

case of an antisymmetric angle-ply laminate. The condition $\delta_{11}\delta_{22} > \delta_{12}^2$ translates into the following inequality:

$$(B_{16}^2 - A_{66}D_{11})(B_{26}^2 - A_{66}D_{22}) > (B_{16}B_{26} - A_{66}D_{12})^2.$$

Regardless of the specific values of B_{ij} and D_{ij}, the left- and right-hand sides of this inequality will be comparable in any material where $B^2 \gg A_{66}D$. In other words, the limit $\det(\boldsymbol{\delta}) \to 0$, which for orthotropic strips can be approached by taking $\beta \to \nu^2$, can be obtained here by increasing the strength of the coupling between stretching and bending. Thus, we might expect angle-ply laminated strips with strong coupling between bending and stretching to be tristable for a broad range of spontaneous curvatures.

5. Conclusions

Despite its relatively long history, the theory of elastic mulitstability is still a field rich in challenging problems and open questions. Most of the theoretical work has been limited to the case of uniform Gaussian curvature deformations. Here, we lift the assumption of uniform curvature variations and inextensibility, and find a variety of morphing and multi-stable scenarios in shells that have both anisotropy and spontaneous curvature. Our results complement and extend those previously reported by Galletly & Guest (2004a,b), Guest & Pellegrino (2006), Seffen (2007) and Vidoli & Maurini (2009). In particular, we emphasize the fundamental role of the intrinsic geometry of the base configuration embodied in the spontaneous Gaussian curvature of the strip. Both strips of positive and negative spontaneous Gaussian curvature admit bistable configurations, but while strips of positive spontaneous curvature are *always* bistable, regardless of the values of the elastic moduli, the occurrence of bistability in strips of spontaneous negative curvature depends crucially on the presence of spontaneous twist as well as the relative stiffness of the strip under tensile and shear deformations. This fundamental difference stems from the fact that the principal curvatures of saddle-like strips can be isometrically switched from positive to negative and vice versa. This leads to the formation of low-energy pathways across the energy barrier corresponding to the flat configuration.

Furthermore, we find that tristability occurs in strip-like plates when $\det(\boldsymbol{\delta}) \sim 0$, where $\boldsymbol{\delta} = \mathbf{D} - \mathbf{B}\mathbf{A}^{-1}\mathbf{B}$ is the effective bending stiffness matrix. In orthotropic materials, this corresponds to the limit $\beta \to \nu^2$, where $\beta = E_y/E_x$ discussed by Vidoli & Maurini (2009) for the case of plates with uniform curvature. A special feature of tristable strips is associated with the height of the barrier separating the two equilibrium configurations of like-sign curvature. The height of this barrier is, in general, much smaller than that associated with the flat configuration. This might have interesting implications for nanoscale materials. Typical strip-like biopolymers, such as proteins or cytoskeletal filaments, have widths of the order of a few nanometres, lengths that range from 1 to 10^3 nm and elastic moduli of the order of mega-Pascal. Assuming $\hat{c}_x$, $\hat{c}_y$ and $\hat{c}_{xy}$ are of order one and $at \sim 1\,\mathrm{nm}^2$, one finds that $U(\kappa_y^-) \approx 3 \times 10^{-4}\,k_\mathrm{B}T\,\mathrm{nm}^{-1}$. Thus, even a micrometre-long strip-like polymer with non-zero spontaneous curvature would be able to fluctuate between minima under the sole effects of thermal excitations. Extending our analysis of

multi-stability to include the effects of thermal fluctuations is likely to yield insights on the dynamical behaviour of biopolymer assemblies and is but one extension of our present analysis.

References

Abdulrahim, M., Garcia, H. & Lind, R. 2005 Flight characteristics of shaping the membrane wing of a micro air vehicle. *J. Aircraft* **42**, 131–137. (doi:10.2514/1.4782)

Ashton, J. E. & Whitney, J. E. 1970 *Theory of laminated plates*, vol. 4. Progress in Materials Science Series. Stamford, CT: Technomic.

Calladine, C. R. 1988 The theory of thin shell structures 1888–1988. *Proc. Inst. Mech. Eng.* (A. E. H. Love Centenary Lecture) **202**, 141–149. (doi:10.1243/PIME_PROC_1988_202_020_02)

Calladine, C. R. 1993 *Theory of shell structures*. Cambridge, UK: Cambridge University Press.

Fernandes, A., Maurini, C. & Vidoli, S. 2010 Multiparameter actuation for shape control of bistable composite plates. *Int. J. Solids Struct.* **47**, 1449–1458. (doi:10.1016/j.ijsolstr.2010.02.007)

Galletly, D. A. & Guest, S. D. 2004a Bistable composite slit tubes. I. A beam model. *Int. J. Solids Struct.* **41**, 4517–4533. (doi:10.1016/j.ijsolstr.2004.02.036)

Galletly, D. A. & Guest, S. D. 2004b Bistable composite slit tubes. II. A shell model. *Int. J. Solids Struct.* **41**, 4503–4516. (doi:10.1016/j.ijsolstr.2004.02.037)

Guest, S. D. & Pellegrino, S. 2006 Analytical models for bistable cylindrical shells. *Proc. R. Soc. A* **462**, 839–254. (doi:10.1098/rspa.2005.1598)

Iqbal, K., Pellegrino, S. & Daton-Lovett, A. 2000 Bi-stable composite slit tubes. In *Proc. IUTAM-IASS Symp. on Deployable Structures, Cambridge, UK, 6–9 September 1998* (eds S. Pellegrino & S. D. Guest), pp. 153–162. Kluwer.

Jones, R. M. 1999 *Mechanics of composite materials*, 2nd edn. Philadelphia, PA: Taylor and Francis.

Kreyszig, E. 1991 *Differential geometry*. New York, NY: Dover Publications.

Lamb, H. 1891 On the flexure of a flat elastic spring. *Phil. Mag* **31**, 182–188. (doi:10.1080/14786449108620096)

Love, A. E. H. 1927 *A treatise on the mathematical theory of elasticity*. New York, NY: Dover Publications.

Mansfield, E. H. 1973 Large-deflexion torsion and flexure of initially curved strips. *Proc. R. Soc. Lond. A* **334**, 279–298. (doi:10.1098/rspa.1973.0092)

Mansfield, E. H. 1989 *The bending and stretching of plates*, 2nd edn. Cambridge, UK: Cambridge University Press.

Mattioni, F., Weaver, P. M., Potter, K. D. & Friswell, M. I. 2007 Analysis of thermally induced multi-stable composites. *Int. J. Solids Struct.* **45**, 657–675. (doi:10.1016/j.ijsolstr.2007.08.031)

Norman, A. D., Seffen, K. A. & Guest, S. D. 2008 Multistable corrugated shells. *Proc. R. Soc. A* **464**, 1653–1672. (doi:10.1098/rspa.2007.0216)

Petroski, H. 2004 Deployable structures. *Am. Sci.* **92**, 122–126. (doi:10.1511/2004.46.3420)

Reissner, E. 1992 On finite twisting and bending of nonhomogeneous anisotropic elastic plates. *J. Appl. Mech.* **59**, 1036–1038. (doi:10.1115/1.2894022)

Rimrott, F. P. J. 1965 Storable tubular extendible member: a unique machine element. *Mach. Des.* **37**, 156–163.

Seffen, K. A. 2007 'Morphing' bistable orthotropic elliptical shallow shells. *Proc. R. Soc. A* **463**, 67–83. (doi:10.1098/rspa.2006.1750)

Seffen, K. A. & Guest, S. D. 2011 Prestressed morphing bistable and neutrally stable shells. *J. Appl. Mech.* **78**, 011002-6. (doi:10.1115/1.4002117)

Vidoli, S. & Maurini, S. 2009 Tristability of thin orthotropic shells with uniform initial curvature. *Proc. R. Soc. A* **464**, 2949–2966. (doi:10.1098/rspa.2008.0094)